AIAA AVIATION Forum
June 27-July 1, 2022, Chicago, IL & Virtual
AIAA AVIATION 2022 Forum

10.2514/6.2022-3724

Multi-Material Topology Optimization for the Conceptual Design of an Additively Manufactured Aerospace Smart Table

Luke Crispo[1], Daniel Krsikapa[2], Kevin Chai[3], Melissa Young[4], and Il Yong Kim[5]
Queen's University, Kingston, Ontario, K7L 3N6, Canada

As the aerospace industry continues to explore advanced lightweighting techniques, topology optimization and additive manufacturing are two key areas that have significant potential but require further research before mainstream adoption. The objective of this work is to perform a multi-material topology optimization study on the design of a business jet smart table fabricated using additive manufacturing. Core optimization theory is reviewed, the smart table design problem is outlined, and the design optimization results are presented. Results indicate that aluminum additive manufacturing should be used in the main structural load paths, while plastic additive manufacturing can provide some stiffness to support minor loads.

I. Introduction

Topology optimization (TO) is a design tool that has seen increased use in the aerospace industry to produce lightweight designs and ultimately drive improved fuel efficiency [1]. TO generates an optimized material distribution from a clean slate design space, resulting in complex designs that can achieve improved performance when compared to size or shape optimization techniques. The application of TO has resulted in weight and/or cost savings in a business aircraft seat [2], a landing gear assembly [3], and an aircraft wing [4]. Multi-material topology optimization (MMTO) is an extension of TO that simultaneously selects between candidate materials and determines the optimal geometry to improve performance compared to a conventional single material design [5].

Additive manufacturing (AM) is a technology that builds a part layer-by-layer instead of traditional subtractive or formative manufacturing methods. This results in nearly unlimited design freedom and presents an opportunity to integrate closely with topology optimization to produce highly complex geometries with minimal interpretation of the optimized structure. MMTO can be used in the conceptual design process to determine where to leverage plastic AM, which is less stiff but cost effective, and metal AM, which has high stiffness but is expensive. Aircraft cabin interiors are highly configurable (especially in business jets) and have several opportunities to begin integrating additive manufacturing [6] without needing to meet the strict design requirements of the primary or secondary aircraft structure.

The objective of this paper is to demonstrate the use of a MMTO design tool for the conceptual design of an aircraft interior component fabricated using AM. First, the underlying MMTO theory will be reviewed. Next, the conceptual design problem of a business jet smart table will be defined. This table will contain integrated electronics, including a display, computer, wireless charger, speaker, and LED lighting, and the structure will be made using entirely aluminum and plastic AM. The MMTO design tool will be applied to the design of the smart table to develop multi-material structures that can accommodate all electronics within a limited design space.

---

[1] PhD Candidate, Department of Mechanical and Materials Engineering.
[2] PhD Student, Department of Mechanical and Materials Engineering.
[3] PhD Student, Department of Mechanical and Materials Engineering.
[4] MASc Student, Department of Mechanical and Materials Engineering.
[5] Professor, Department of Mechanical and Materials Engineering.

II. Multi-Material Topology Optimization

Density-based topology optimization builds on the finite element method by assigning a density design variable to all elements in the design space and interpolating material properties using the solid-isotropic material with penalization (SIMP) interpolation scheme [7]. The material existence design variable, ρ_e^1, can vary between zero (corresponding to a void element) and one (corresponding to a solid element) with a penalty factor used to discourage intermediate densities from occurring in the final optimized solution. MMTO introduces a second design variable per element, ρ_e^2, the material selection design variable, and interpolates element stiffness as

$$E_e\left(\rho_e^1, \rho_e^2\right) = \left(\rho_e^1\right)^p \left(E^2 + \left(\rho_e^2\right)^p \left(E^1 - E^2\right)\right) \tag{1}$$

where E_e is the interpolated Young's modulus, p is the SIMP penalty factor, and E^1 and E^2 are the stiffnesses of material one and material two, respectively. For solid elements (with $\rho_e^1 = 1$), a material selection design variable value of one corresponds to an element stiffness of material one, while a value of zero corresponds to the stiffness of material two.

The MMTO problem statement shown in Eq. (2) will be used in this work to minimize the compliance, C, of the structure subject to a linear static governing equation where $\underset{\sim}{K}$ is the global stiffness matrix, $\underset{\sim}{u}$ is the vector of nodal displacements, and $\underset{\sim}{f}$ is the vector of applied forces. The optimization is constrained by two volume fraction constraints, $g_k(\underset{\sim}{\rho})$, where $\bar{V}_1$ is volume fraction limit of any material to be used, $\bar{V}_2$ is the volume fraction limit of first material defined, and V_e is the volume of the *e*-th element.

$$\begin{aligned}
&\text{minimze} \quad && C\left(\underset{\sim}{\rho}\right) = \underset{\sim}{f}^T \underset{\sim}{u}\left(\underset{\sim}{\rho}\right) \\
&\text{subject to} \quad && \underset{\sim}{K}\underset{\sim}{u} = \underset{\sim}{f} \\
& && g_k\left(\underset{\sim}{\rho}\right) = \frac{\sum_e \left[V_e \prod_{j=1}^{k} \rho_e^j\right]}{\sum_e V_e} \le \bar{V}_k, \quad k = 1,2 \text{ materials} \\
& && \forall \text{ element } e,\ \rho_e^k \in (0,1], \quad k = 1,2 \text{ materials}
\end{aligned} \tag{2}$$

The optimization problem is solved iteratively using the method of moving asymptotes (MMA) [8] optimization algorithm implemented in a custom Fortran code using Altair OptiStruct [9] software to solve the linear static analysis. Sensitivity expressions are needed for any gradient-based optimization solver, and the MMTO objective and constraint sensitivities have been derived by Li and Kim [5]. The objective sensitivities are outlined below with respect to both design variable values in Eq. (3) - (4), where C_e is the element level compliance calculated by OptiStruct.

$$\frac{\partial C}{\partial \rho_e^1} = \frac{-p}{\rho_e^1} C_e \tag{3}$$

$$\frac{\partial C}{\partial \rho_e^2} = \frac{-p}{\rho_e^2}\left(1 - \frac{E^2}{E^2 + \left(\rho_e^2\right)^p \left(E^1 - E^2\right)}\right) C_e \tag{4}$$

The two constraint function sensitivities are shown below in Eq. (5) and (6). The first constraint limits the material existence design variable and therefore has a sensitivity value of zero with respect to the material selection design variable. The second constraint limits the volume of material one (calculated as $\rho_e^1 \rho_e^2$) and therefore has sensitivity expressions for both design variables.

$$\frac{\partial g_1}{\partial \rho_e^1} = \frac{V_e}{\sum_e V_e}, \qquad \frac{\partial g_1}{\partial \rho_e^2} = 0 \tag{5}$$

$$\frac{\partial g_2}{\partial \rho_e^1} = \frac{\rho_e^2 V_e}{\sum_e V_e}, \qquad \frac{\partial g_2}{\partial \rho_e^2} = \frac{\rho_e^1 V_e}{\sum_e V_e} \tag{6}$$

Objective and constraint sensitivities are filtered using the mesh-independent filter [10] to prevent the checkerboarding phenomena from occurring. Equation (7) calculates the filtered sensitivity of a generic objective or constraint, $(\partial\Phi/\partial\rho_i^j)^*$, based on element densities and unfiltered sensitivities, $\partial\Phi/\partial\rho_i^j$, of the N neighbouring elements in a sphere of radius r around the central element. The H_i term defined in (8) is calculated as the distance between the *e*-th central element and the *i*-th neighbouring element. In this work, the filter radius was set to 1.5 × the average mesh size of the design space.

$$\left(\frac{\partial\Phi}{\partial\rho_e^j}\right)^* = \frac{1}{\rho_e^j \sum_{i=1}^{N} H_i} \sum_{i=1}^{N} \left(H_i \rho_i^j \frac{\partial\Phi}{\partial\rho_i^j} \right) \tag{7}$$

$$H_i = \max\left\{0, r - \text{distance}(e,i)\right\} \tag{8}$$

III. Smart Table Design Study

The cabin interior design is a major feature for business jets, leading manufacturers to integrate electronic components throughout the cabin to enhance user experience. For example, the Bombardier Global 7500 has an integrated OLED display dial in the sideledge, a suite controller in the cabin divider, and a 4k home theatre [11]. This project aims to integrate electronic components into a smart table that can be stowed beneath the sideledge. The conceptual table design in this work will contain a display, a wireless charger, an internal computer, speakers, and LED accent lighting. Additive manufacturing and topology optimization are ideal technologies to explore in the fabrication of the smart table because they allow for complex internal structures that provide stiffness within a thin design space, while easily facilitating space for the internal components and their wiring. Connections between electronics and the structure can also easily be designed and manufactured with AM. This work will explore the conceptual design of the internal stiffening structure of the smart table considering both aluminum and plastic AM using MMTO. Other design aspects to be addressed in future work include efficient packaging of electronics, printability of the AM components, and lattice structure optimization.

A. Finite Element Model

Before conducting topology optimization, a finite element model must be created to specify the structural loading, non-designable geometry, and designable region for optimization. Fig. 1 shows the model used in this work for a 27" x 27" x 0.89" table that folds about its midplane in the longitudinal axis of the aircraft. Three generic hinges connect the two folding leaves of the table, which are separated by 1mm. The outboard leaf is attached to two support arms that are fixed at two attachment points within the dado panel. The support arms are fixed in all degrees of freedom on the top surface at the outboart point and are fixed in the y degree of freedom on the bottom surface as indicated in Fig. 1. The support arms are solid and non-designable regions in this work but will be optimized in the future. Five loads are applied to the table in separate load steps: Corner 1, Corner 2, Edge, Side 1, and Side 2. RBE3 elements are used to distribute the point loads over a defined area.

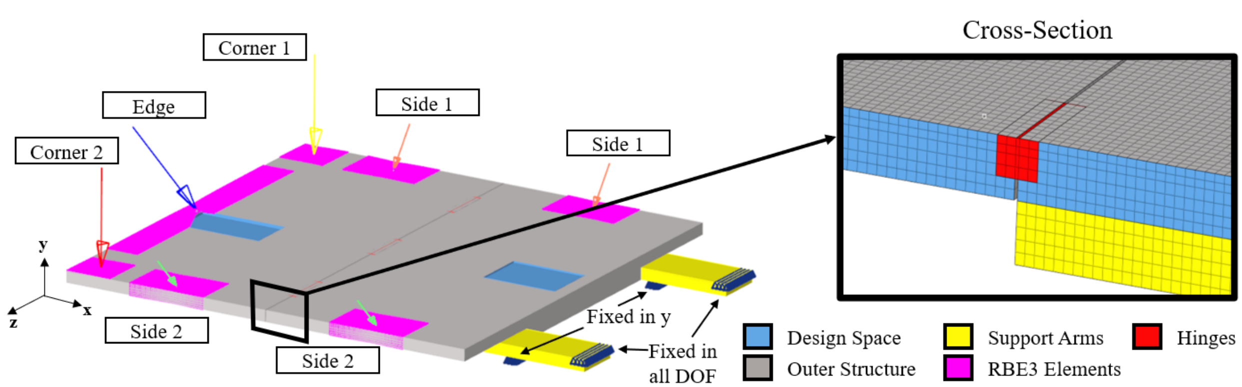

Fig. 1 Finite element model of smart table with design and non-design space. Loads are indicated with arrows and constraints with triangles.

The outer surfaces of the table (i.e., the top, bottom, and side table surfaces) will be manufactured using plastic AM covered with a veneer finish. The 4mm thick outer surface has a fixed geometry and is modelled using 2D plate elements that are connected directly to the internal design space composed of approximately 360,000 solid elements. It should be noted that the direct connection of the 2D plate to 3D solid elements over-stiffens the structure because half of the thickness of plate elements is overlapping with the solid elements. This compromise was made to reduce computing time compared to modelling the entire structure with solid elements. Cutouts were removed from the design space for a 5.5” display in the inboard leaf and a wireless charger in the outboard leaf as these two components have fixed, predetermined locations selected based on ergonomic and functional criteria. Other internal components (computer, speakers, and wiring) were not considered in the design space as their location can be adjusted based on the topology optimization results. The finite element model had about 510,000 elements overall.

The MMTO problem had the option to use both aluminum and plastic AM in the internal design space. The material properties of each component used in the smart table design are summarized in Table 1. The aluminum and Bayblend will be additively manufactured, while the hinges are made of generic stainless steel. All materials were assumed to have Poisson’s ratio of 0.3.

Table 1 Material properties used in smart table optimization

Material	Young’s Modulus [GPa]	Density [g/cm^3]	Components
AlSi10Mg [12]	70	2.67	design space, support arms
Bayblend FR410 MT* [13]	2.96	1.30	design space, outer structure
Stainless Steel	200	7.80	hinges

*Stiffness of the plastic material is weakened by 25% to account for the unknown properties when printing with AM.

B. Optimization Results

Topology optimization can be solved with a variety of problem statements, considering objectives such as mass or cost, and constraints including displacement, stress, and natural frequencies. For preliminary conceptual design purposes, a compliance objective function is a good starting point to quickly determine optimized material layouts for various mass or volume fraction limits.

In this work, to investigate the impact of aluminum and plastic material use in the smart table internal structure, the MMTO problem statement was solved for a range of volume fraction constraints. The aluminum volume fraction constraint ($\bar{V}_2$) was limited to 1%, 2%, 2.5%, 3%, and 5% aluminum, with four variations of total volume fraction constraint in each respective case, resulting in 20 MMTO iterations. In addition, single material TO was solved for 3 different volume fractions of aluminum-only and plastic only design spaces. Constraint levels were selected arbitrarily to explore a wide range of material distributions and to yield optimized structures with similar displacement values. All studies minimized the weighted sum of compliance for all applied loads. The optimization computational time was approximately 5 hours for MMTO and 2 hours for single material TO running on a Windows PC (16 cores, 3.5 GHz, 128 GB RAM).

Optimization results are summarized in Fig. 2, showing a contour plot of the material ID for each element. Note that the shell elements representing the table surface were hidden in the figures to better view the internal structure. The single material aluminum TO resulted in web-like structures extending from the outer hinges to the inboard corners of the table, where the corner loads are applied. Plastic-only optimizations resulted in a hollow shell structure in the inboard leaf with reinforcements along the support arms in the outboard leaf. All MMTO designs had the same aluminum features branching out from the hinges to the applied loads at the inboard corners of the table. The optimizer distributed plastic in varying degrees to other areas of the table to provide general increases in stiffness. These features agree with intuition as the aluminum material has a significantly higher stiffness/density ratio and should therefore be placed in the main load paths of the table.

A Pareto frontier of the compliance and mass (competing responses in the optimization) of all designs is plotted in Fig. 3. Multi-material designs are grouped according to the aluminum volume fraction constraint limit indicated in the legend. The Pareto frontier indicated by the dashed line shows that as expected, a decrease in mass is generally associated with an increase in compliance. This trend is also apparent between designs with the same volume fraction of aluminum but does not occur across designs with different volume fractions of aluminum. Multi-material designs with little plastic usage (5%, 3%, and 2.5% aluminum volume fractions) were comparable to aluminum only designs, while designs with high amounts of plastic (2%, 1%, and 0% aluminum volume fractions) performed poorly in terms of the assessed objectives. In particular, the plastic-only designs were 2 times heavier compared to aluminum only designs with similar compliance values. These findings indicate that for the smart table design, the main structural components should be composed of aluminum, while plastic should be used sparingly to provide support in less critical areas.

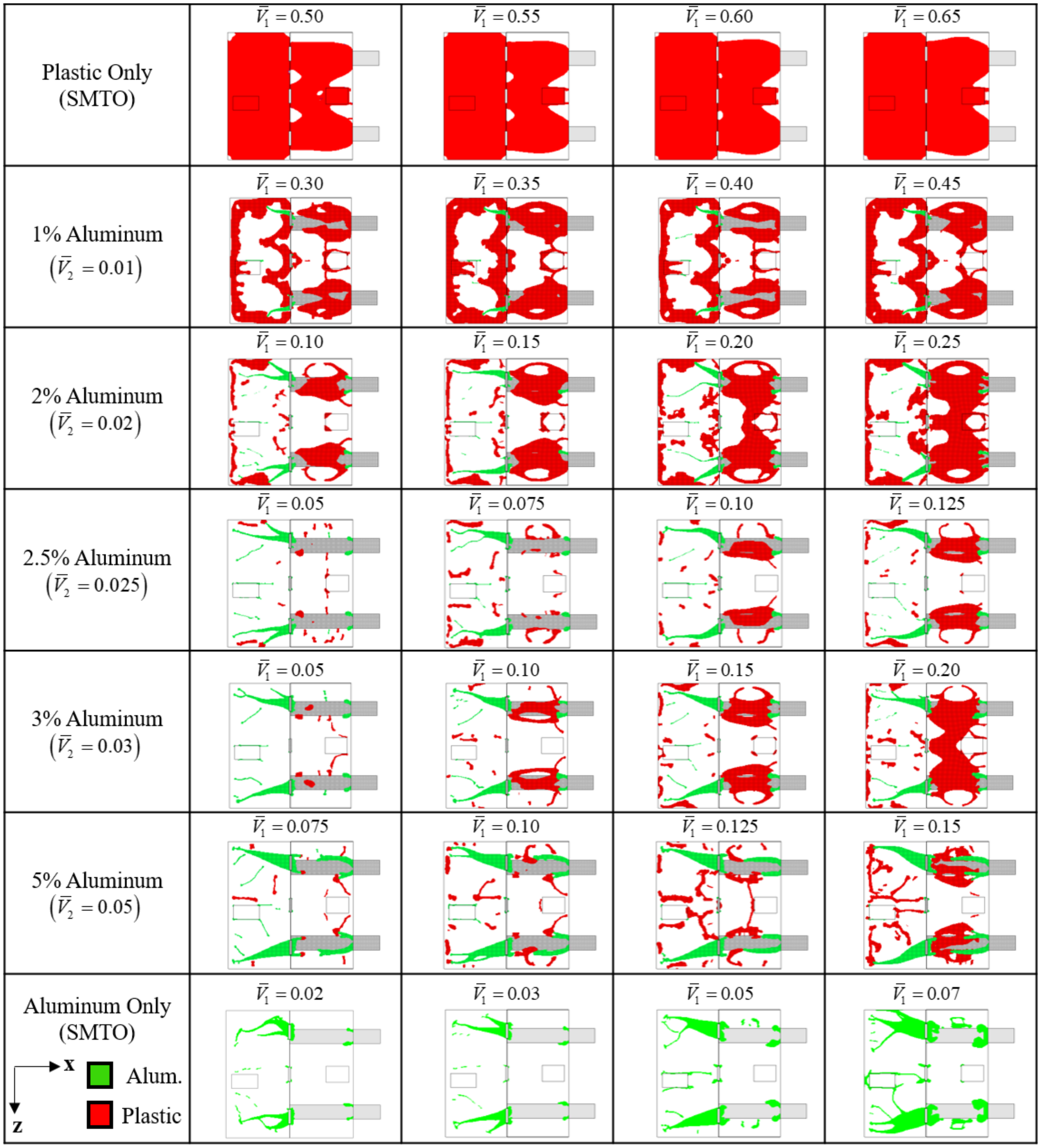

Fig. 2 Summary of topology optimization results for various volume fraction constraints. Each row represents a different aluminum volume fraction (in MMTO) and each column represents a different total volume fraction.

The conceptual design process is typically followed by an in-depth design stage on a single (or a set of) optimized result(s), conducting topology, size, and shape optimization to further refine the design. In this work, the multi-material solution with 2.5% aluminum and 2.5% plastic (5% overall volume fraction) shown in Fig. 4 was identified to be pursued for further design optimization, which will be conducted in future research.

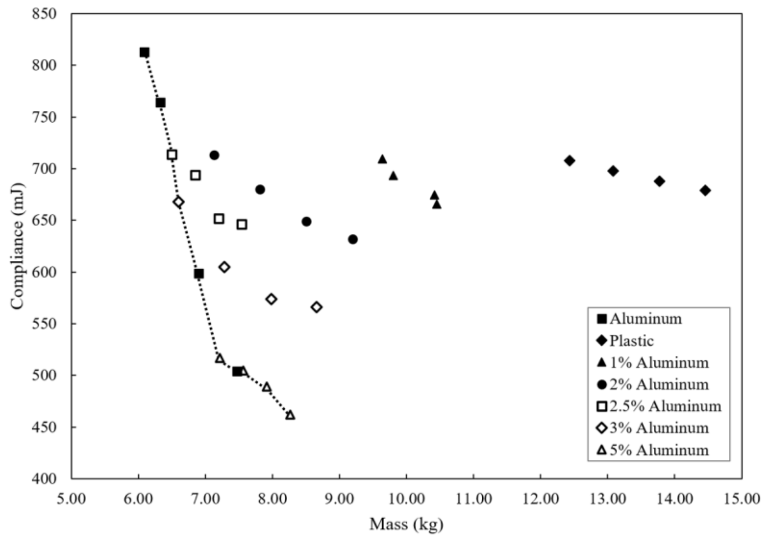

Fig. 3 Pareto frontier trade-off study between compliance and mass for smart table MMTO.

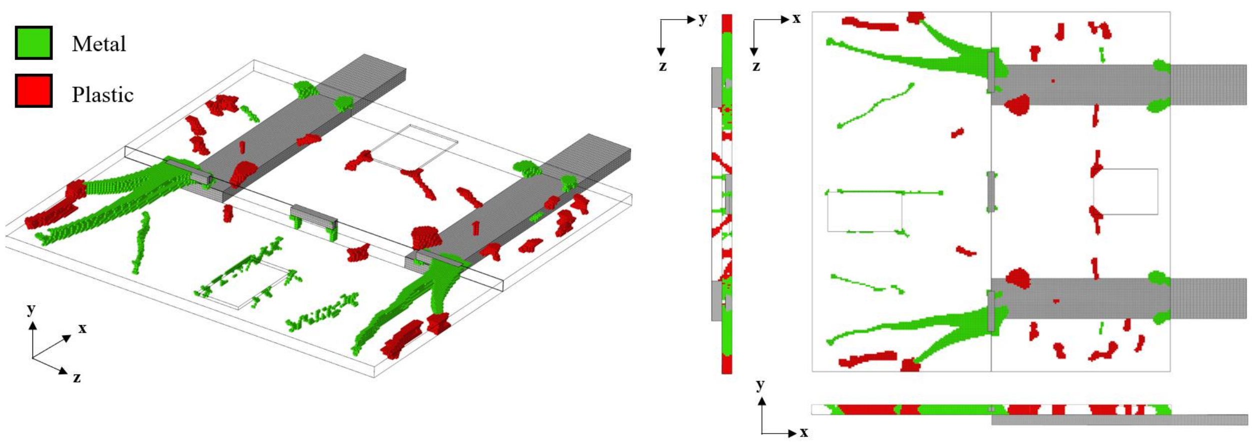

Fig. 4 Multi-material conceptual design to be considered in future work.

IV. Conclusion

This paper outlines an approach for using multi-material topology optimization in the conceptual design of an aircraft interior component manufactured with additive manufacturing. The MMTO problem statement allows designers to generate optimized structures for specified volume fractions of any two materials. This enables easy design exploration, as demonstrated on the smart table case study. Results of the conceptual design study were plotted and compared in terms of compliance and mass, with only a small portion of the designs existing on the optimal Pareto frontier. Readers are strongly recommended to explore different ratios of materials when implementing a multi-material design, to ensure that a strong optimized design is achieved. In this application, designs using large amounts of plastic performed significantly worse relative to other designs. Some design features were consistent between all optimized solutions, such as the placement of aluminum from the hinges to the inboard corners of the table, indicating that these features contribute greatly towards stiffness of the structure.

In the future, adjustments to the model can be made to improve the accuracy of finite element analysis. Potential improvements include modelling hinges and support arms more accurately and considering connection points between components. From an optimization perspective, the problem statement could be updated to minimize mass subject to key design requirements, such as stress and deflection limits. The presented MMTO methodology assumes that dissimilar materials are perfectly bonded together, overestimating the stiffness of the design. A multi-material and multi-joint topology optimization approach would result in a more realistic design by considering connections between different materials and including joining cost as a response during the optimization [14].

Moving forward, the design freedom of AM could be leveraged to generate designs with further performance improvements. A plastic lattice structure could be added as a third material option in MMTO with a lower stiffness and density compared to the fully solid plastic material. Lattice structure optimization could also be implemented to continuously vary the plastic lattice structure throughout the table design space. Finally, design for additive manufacturing and part consolidation theory should be integrated into the multi-material topology optimization algorithm to produce optimized designs that are readily manufacturable and cost effective for AM techniques [15].

Acknowledgments

This research was funded by the Natural Sciences and Engineering Research Council of Canada (NSERC) and industry partner Bombardier Inc. Special thanks to Bruce Malek, Lubomir Trendafilov, and Sehrish Waseem. Their expertise was greatly appreciated.

References

[1] Zhu, J. H., Zhang, W. H., and Xia, L., "Topology Optimization in Aircraft and Aerospace Structures Design," *Archives of Computational Methods in Engineering*, Vol. 23, No. 4, Dec. 2016, pp. 595-622.
doi: 10.1007/s11831-015-9151-2

[2] Trivers, N., Carrick, C., and Kim, I. Y., "Design optimization of a business aircraft seat considering static and dynamic certification loading and manufacturability," *Structural and Multidisciplinary Optimization*, 2020, pp. 20.
doi: 10.1007/s00158-020-02650-z

[3] Wong, J., Ryan, L., and Kim, I. Y., "Design optimization of aircraft landing gear assembly under dynamic loading," *Structural and Multidisciplinary Optimization*, Vol. 57, No. 3, Mar. 2018, pp. 1357-1375.
doi: 10.1007/s00158-017-1817-y

[4] Kashanian, K., and Kim, I. Y., "A novel method for concurrent thickness and material optimization of non-laminate structures," *Structural and Multidisciplinary Optimization*, Vol. 64, No. 3, Sep. 2021, pp. 1421-1437.
doi: 10.1007/s00158-021-02928-w

[5] Li, C., and Kim, I. Y., "Multi-material topology optimization for automotive design problems," *Proceedings of the Institution of Mechanical Engineers Part D: Journal of Automobile Engineering*, Vol. 232, No. 14, Dec. 2018, pp. 1950-1969.
doi: 10.1177/0954407017737901

[6] Stratasys Direct, I., "Top 3 Ways 3D Printing is Transforming Aircraft Interiors," url: https://www.stratasysdirect.com/industries/aerospace/3d-printing-transforming-aircraft-interiors [retrieved 8 October 2021].

[7] Bendsoe, M. P., and Sigmund, O., *Topology Optimization: Theory, Methods, and Applications*, Springer Berlin Heidelberg, pp. 370

[8] Svanberg, K., "The Method of Moving Asymptotes - a New Method for Structural Optimization," *International Journal for Numerical Methods in Engineering*, Vol. 24, No. 2, Feb. 1987, pp. 359-373.
doi: 10.1002/nme.1620240207

[9] Altair, "Altair OptiStruct 2019 User Guide," Altair Engineeering Inc., 2019

[10] Sigmund, O., "Morphology-based black and white filters for topology optimization," *Structural and Multidisciplinary Optimization*, Vol. 33, Apr. 2007, pp. 401-424.
doi: 10.1007/s00158-006-0087-x

[11] Bombardier, "The nice Touch cabin management system," url: https://businessaircraft.bombardier.com/en/global-7500/nice-touch-cms [retrieved 13 October 2021].

[12] EOS, "EOS Aluminium AlSi10Mg," EOS GmbH – Electro Optical Systems, 2018

[13] Covestro, "Bayblend FR410 MT ISO Datasheet," Covestro AG, 2018

[14] Crispo, L., Roper, S. W. K., Bohrer, R., Morin, R., and Kim, I. Y., "Multi-Material and Multi-Joint Topology Optimization for Lightweight and Cost-Effective Design," *ASME 2021 International Design Engineering Technical Conferences and Computers and Information in Engineering Conference*, Vol. 3B: 47th Design Automation Conference (DAC), 2021.

[15] Crispo, L., and Kim, I. Y., "Part consolidation for additive manufacturing: A multilayered topology optimization approach," *International Journal for Numerical Methods in Engineering*, 2021, pp. 41.
doi: 10.1002/nme.6754